

# Combined Bowtie–Peano Antennas for Wideband Performance

**Ioannis I. Papadopoulos-Kelidis, Antonios X. Lalas,  
Nikolaos V. Kantartzis, and Theodoros D. Tsiboukis**

Department of Electrical and Computer Engineering  
Aristotle University of Thessaloniki, Thessaloniki, GR-54124, Greece  
gianniskelidis@yahoo.gr, lant@faraday.ee.auth.gr, kant@auth.gr, tsiboukis@auth.gr

**Abstract** — The concept of the folded bowtie wideband antennas is introduced in this paper. To this aim, the design procedure employs a Peano space-filling curve approach which leads to an entire family of combined bowtie-Peano antennas (BPA). The new structures efficiently blend the broadband performance of bowtie antennas with the compactness of Peano forms. In this context, two alternative devices are proposed and thoroughly investigated. Numerical results derived by means of a finite-difference time-domain (FDTD) technique clearly reveal the behavior and the merits of the novel radiators, signifying, also, the feasibility of bandwidth enhancement at specific resonances.

**Index Terms** — Bowtie antennas, FDTD methods, miniaturized antennas, Peano antennas.

## I. INTRODUCTION

An issue of paramount significance in contemporary RF technology is the multi-parametric design of highly competent and reliable antennas. When embedded in wireless networks or advanced communication systems, these structures are expected to exhibit various benefits, like compactness combined with functionality in lower frequencies, irrespective of their physical size. The primary idea for the accomplishment of the prior features at a single antenna is to fold a dipole in such a manner that fits into a small area, yet preserving its resonances at the same frequency regions. From this viewpoint, space filling curves [1-5] can be utilized to meet these requirements and effectively tackle any shortcomings of the design process. Among them, Peano antennas [6-8] comprise a practical and proficient selection with

respect to high compression ratio. In fact, their small electrical size associated with a satisfactory multi-band behaviour can easily justify their noteworthy contribution in diverse applications.

Of critical essence, as well, is the wideband performance of wireless RF apparatuses. A popular structure for broadband designs is the bowtie antenna [9-11]. Although, its overall operation resembles that of a dipole, this particular radiator attains a sufficiently enhanced bandwidth. On the other hand, careful research on this aspect has confirmed that Peano space-filling curves can lead to miniaturized configurations with acute, but narrowband, resonances [12-14]. As a consequence, it becomes apparent that the combination of the preceding concepts is likely to provide adequately wideband and noticeably compact devices, which meet all modern antenna functional standards.

It is the objective of this paper to elaborately examine the radiation characteristics of efficient bowtie structures folded in terms of the Peano space-filling curve. Two novel antennas are carefully designed in order to merge the desired attributes of the aforementioned designs. In the first case, a bowtie-shaped metallic path is introduced, while in the latter the outline of Peano's footprint is transformed into a bowtie shape. The performance of the combined bowtie-Peano antennas (BPA) is numerically studied via a finite-difference time-domain (FDTD) scheme and compared to that of a typical Peano antenna, considering the multiple resonances of both devices. Analysis proves that the proposed structures achieve notably improved bandwidths with very limited dimensions.

## II. CONVENTIONAL PEANO ANTENNA

Space filling curves constitute a mathematical conception for the compression of a straight line

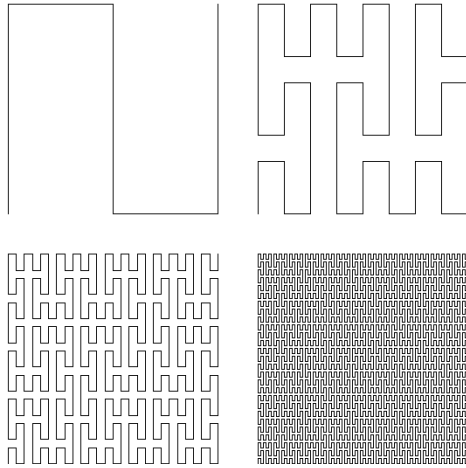


Fig. 1. Geometry of the Peano curves for the first four iteration orders.

into a restricted area. A well-known representative is the Peano curve, shown in Fig. 1 for the first four iteration orders. Specifically, a Peano space filling curve is considered as a map from the unit interval  $I = [0,1]$  to the unit area  $Q = [0,1]^2$ . Hence, each point of  $I$ , signified in the decimal system, is transformed into its ternary equivalent by

$$(0.t_1t_2\dots)_3 = (t_13^{-1} + t_23^{-2} + \dots)_{10}, \quad (1)$$

where the  $t_j = 0,1,2$  denote ternary digits. Then, this number is mapped to a point of  $Q$  through the application of function

$$f_p((0.t_1t_2t_3\dots)_3) = \begin{pmatrix} (0.t_1(k^{t_2}t_3)(k^{t_2+t_4}t_5)\dots)_3 \\ (0.(k^{t_1}t_2)(k^{t_1+t_3}t_4)\dots)_3 \end{pmatrix}, \quad (2)$$

along with operator  $k$ , defined as

$$kt_j = 2 - t_j, \quad (3)$$

with  $k^v$  the  $v$ -th iterative enforcement of  $k$ . Finally, all coordinates represented in the ternary system are transformed into their decimal counterparts.

Implementing the above algorithm and bearing in mind the fundamental properties of space compression, it is feasible to design specific antennas with a high level of compactness. The topology of the antenna studied, herein, is a top-loaded monopole, exploiting the 2<sup>nd</sup> order Peano curve to form a metallic path, as depicted in Fig. 2a. The whole

structure is placed above a ground plane according to the arrangement of Fig. 2b. The device is excited via the probe of a coaxial cable connected to the center of the curve, while two cylindrical shorting posts connect the end-points of the antenna to the

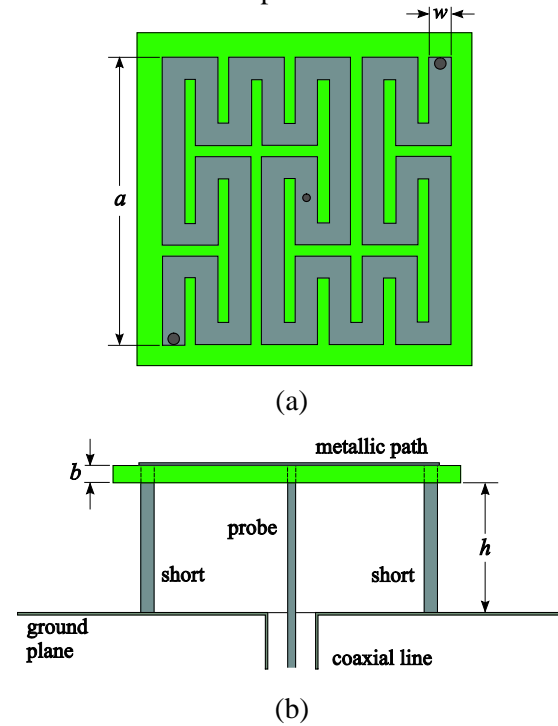


Fig. 2. Top-loaded monopole Peano antenna. (a) metallic path geometry and (b) side perspective.

ground. In this framework, based on the gamma match excitation of dipoles [15], a matching network to a  $50 \Omega$  source is created, without the need of any external apparatus.

The metallic path of the antenna is constrained on a  $19.1 \text{ mm} \times 19.1 \text{ mm}$  footprint, whereas path width  $w$  is, respectively, set to  $1.49 \text{ mm}$  and  $2.11 \text{ mm}$  for the two designs under investigation. A  $1.5 \text{ mm}$  thick substrate with a dielectric permittivity of  $2.21$  is selected to provide the appropriate mechanical support to the antenna. Moreover, the distance between the substrate and the ground plane is set to  $h = 8.5 \text{ mm}$ , while the radius of the cylindrical shorting posts is  $r = 0.5 \text{ mm}$ . For our simulations, a 3-D FDTD technique in conjunction with a 6-cell perfectly matched layer (PML) absorber for open-boundary termination [16], is developed. In view of these structural data, a detailed parametric study is conducted regarding the substrate's height and the radius of the shorting posts. Actually, the role of these two parameters in the

achievement of the correct matching and the desired behavior is deemed decisive. From the analysis, it is evident that, when  $h$  increases (Fig. 3a) or  $r$  decreases (Fig. 3b), a shift of the  $S_{11}$  parameter towards lower frequencies occurs. Also, to obtain a more general view of the antenna's operation, its surface current distribution at the frequency of 2.52 GHz is illustrated in Fig. 4, in which minimum values are observed near the center of the device.

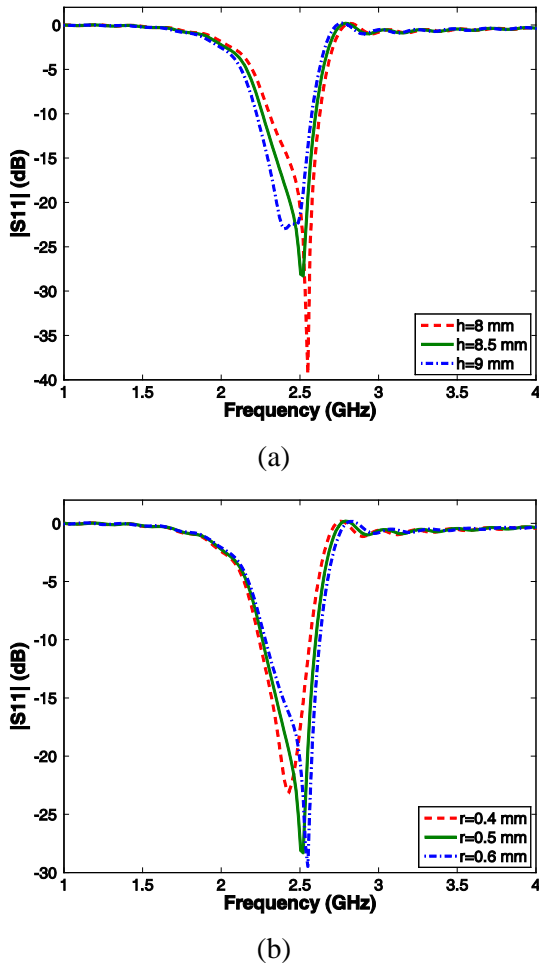


Fig. 3. Variation of the  $S_{11}$  parameter for different values of (a) the substrate's height and (b) the radius of the shorting posts.

### III. COMBINED BPA CONFIGURATION

The broadband behavior of the bowtie antenna (Fig. 5a) can be exploited to circumvent the bandwidth restrictions of the conventional Peano structures. The proposed configuration according to the folded bowtie concept is shown in Fig. 5b, where modifications have been conducted only at the bowtie shaped metallic path. In this context, slope

$s$ , describing the tangent of the bowtie's angle, is introduced as an additional parameter to distinguish the new device from the conventional one. Here,  $s$  is set to 0.0035, while the width of the initial path is 1.49 mm. Therefore, the final value of  $w$  is 2.11 mm in order to enable comparisons with the aforementioned Peano designs.

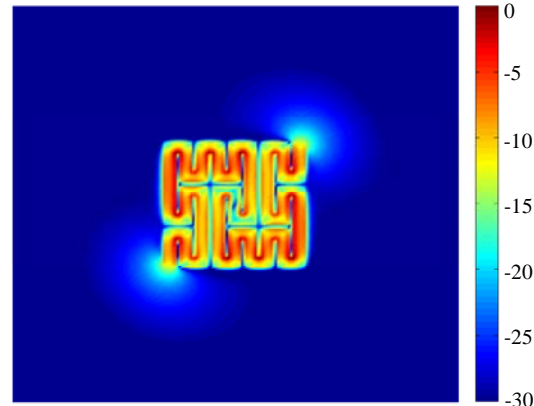


Fig. 4. Surface current distribution of the Peano antenna at the frequency of 2.52 GHz.

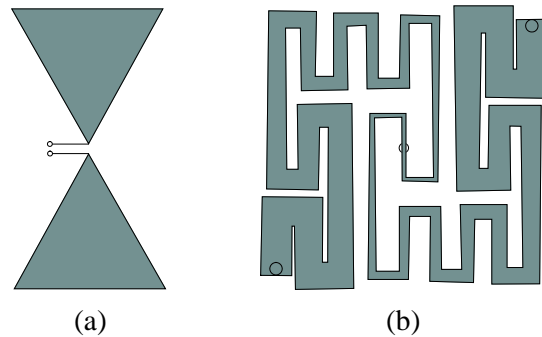


Fig. 5. Geometry of (a) the bowtie antenna, and (b) the metallic path of the combined BPA.

To this goal, Fig. 6 performs a comparison between two conventional Peano designs and the combined BPA through the variation of the  $S_{11}$  parameter. Furthermore, the spectral features of the three radiating arrangements are summarized in Table 1. As deduced, in contrast to the Peano antenna with the smaller path width, the BPA presents a significantly enhanced bandwidth (7 times broader) at the resonant frequency of 10.26 GHz, whereas the fundamental resonance vanishes. In addition, a frequency shifting of roughly 1 GHz is observed for the BPA. On the other hand, when comparing the BPA with the other Peano antenna, an improved bandwidth (3 times broader) is discerned at the resonant frequency of 4.755 GHz

along with a frequency shifting, while a new resonance at 10.26 GHz is revealed, achieving a bandwidth of 0.192 GHz. Thus, the novel BPA can offer an enhanced wideband performance, with the undesirable frequency shifting tackled by properly modifying its design parameters.

Proceeding with our study, the surface current distributions of the combined BPA at the extra resonances of 4.755 GHz and 10.26 GHz are shown in Fig. 7. Finally, Fig. 8 depicts the radiation patterns of all structures at certain resonant frequencies. It is apparent that minor deviations are introduced by the BPA arrangement. Nevertheless, its maximum gain is slightly decreased. Particularly, the BPA exhibits a gain of 4.4 dB at 4.755 GHz versus the 6.3 dB at 5.715 GHz of the conventional antennas (Fig. 8a). Also, a gain of 6.4 dB at 10.26 GHz in opposition to the 7.8 dB at 10.2 GHz is observed in Fig. 8b.

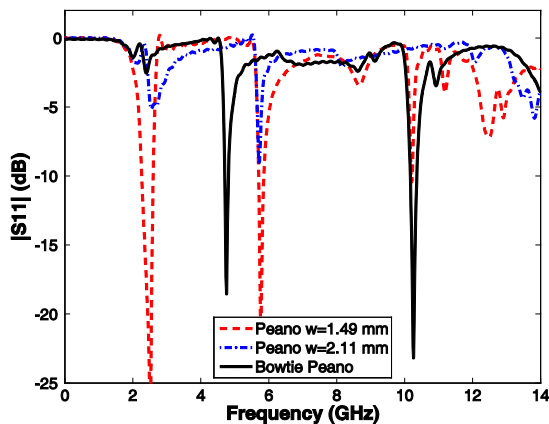
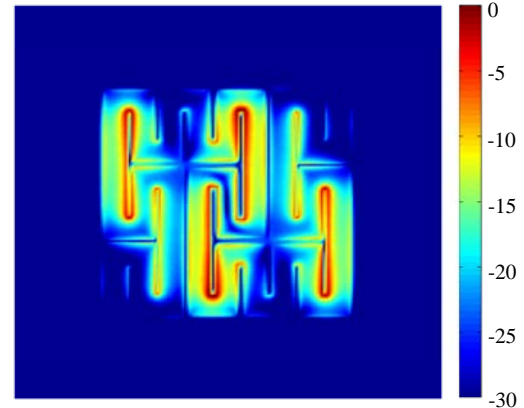


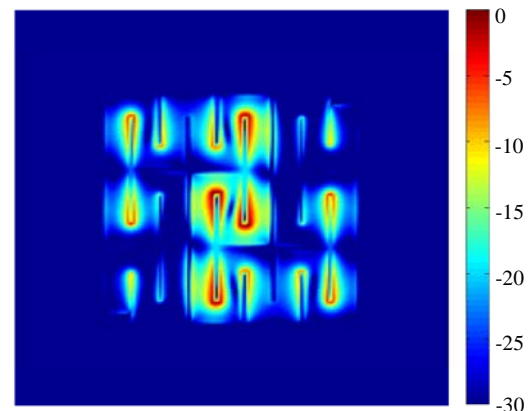
Fig. 6. Variation of the  $S_{11}$  parameter: Conventional Peano designs versus the proposed BPA.

Table 1: Bandwidth comparison (at -10 dB) of various Peano antennas for two resonances

Antenna	Res.	Start (GHz)	End (GHz)	BW (GHz)
Peano $w = 1.49$ mm	2 <sup>nd</sup>	5.704	5.855	0.151
	3 <sup>rd</sup>	10.192	10.220	0.028
Peano $w = 2.11$ mm	2 <sup>nd</sup>	5.692	5.746	0.054
	3 <sup>rd</sup>	—	—	—
Proposed BPA	2 <sup>nd</sup>	4.690	4.838	0.148
	3 <sup>rd</sup>	10.164	10.356	0.192



(a)



(b)

Fig. 7. Surface current distribution of the BPA configuration at (a) 4.755 GHz and (b) 10.26 GHz.

#### IV. ALTERNATIVE BPA DESIGN WITH A BOWTIE OUTLINE

In contrast to the radiating arrangement of the previous section, which is implemented by a bowtie shaped metallic path, the antenna designed, herein, presents a constant path width of  $w = 1.5$  mm. However, the outline of its footprint is altered into a bowtie frame prescribed by an angle of  $2\varphi$  ( $\varphi = 22^\circ$ ), as illustrated in Fig. 9. The feed of the device remains the same, separating the structure into two sub-antennas, the end-points of which are denoted from the corners of the Peano curve at the shorting posts and the center of the coaxial probe. Note that angle  $2\varphi$  introduces an asymmetry in the dimensions of the two sub-devices and hence the two parts of the metallic path have different lengths. In spite of angle  $2\varphi$  and the consequent change of the footprint's shape, the area occupied is identical. So, a comparison with the conventional antenna of the same footprint can be readily performed.

Additionally, the height of the substrate measured from the ground plane is  $h = 16$  mm, the substrate thickness is  $b = 1.5$  mm, and its dielectric permittivity is 2.21 to achieve the proper matching.

To comprehend the role of the modification in the alternative BPA, Fig. 10 presents the impact of the substrate’s height, the radius of the shorting posts, and the angle. Notice that matching as well as the desired performance is attained, while a shift towards lower frequencies is observed, as  $h$  increases or  $r$  decreases. Also, as  $\varphi$  decreases, the two distinct resonances get closer and tend to merge. Next, a comparison between the conventional Peano antenna and the alternative BPA design is attempted. Hence, Fig. 11 gives the variation of the  $S_{11}$  parameter and Table 2 summarizes the spectral characteristics of the resonant frequencies. From the results, the alternative BPA reveals a clear separation of the conventional Peano’s first resonance into two adequately deep discrete regions. This can be mainly attributed to the asymmetry in the dimensions of the two sub-antennas. So, different path lengths lead to two distinct resonances. Also, the alternative BPA presents an enhanced bandwidth (6 and 4 times broader) at the resonant frequencies of 7.365 GHz and 8.04 GHz, respectively, in contrast to the typical Peano configuration. However, a reduced bandwidth is observed at the resonant frequencies of 1.575 GHz and 9.9 GHz. This minor discrepancy can be basically attributed to the asymmetry introduced by the alternative arrangement. Nevertheless, the majority of the resonances retain their enhanced performance. Hence, it is derived that the alternative BPA can attain an improved wideband behavior through the tuning of its design parameters.

Concerning the radiation performance of the alternative BPA, Fig. 12 displays its surface current distribution at the resonant frequency of 1.575GHz. Recalling the results of Table 2, a gain enhancement is deduced at all resonant frequencies. In addition, Fig. 13 compares the radiation patterns of a conventional Peano and the proposed antenna at specific resonant frequencies. Expressly, the alternative BPA attains a gain of 4.2 dB at 1.905 GHz versus the 3 dB at 1.86 GHz of the typical Peano device (Fig. 13a). Moreover, a gain of 10.2 dB at 8.04 GHz as opposed to the 7.8 dB at 8.265 GHz is detected in Fig. 13b. Finally,

the shapes of the radiation patterns are not seriously modified despite the geometrical changes.

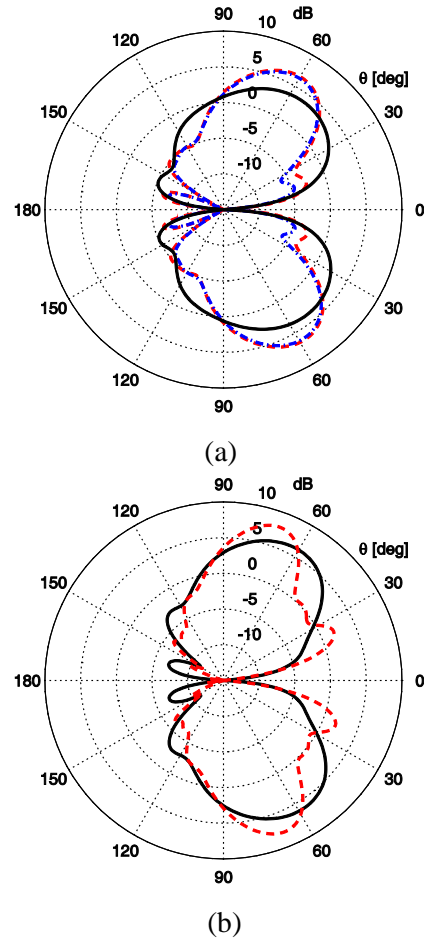


Fig. 8. Gain radiation patterns at  $\varphi = 135^\circ$  of conventional Peano designs versus the combined BPA: (a) Resonances at 5.76 GHz, 5.715 GHz, 4.755 GHz (red:  $w = 1.49$  mm, blue:  $w = 2.11$  mm, black: BPA) and (b) resonances at 10.2 GHz, 10.26 GHz (red:  $w = 1.49$  mm, black: BPA).

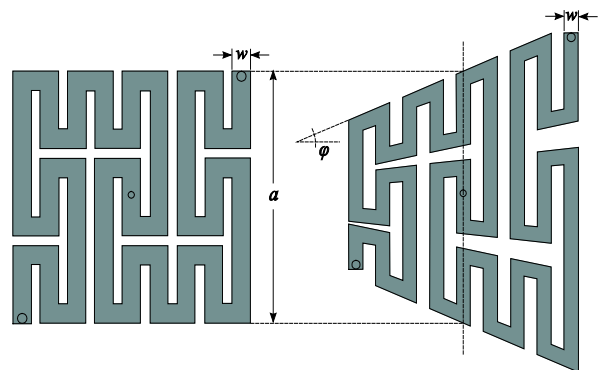


Fig. 9. Geometry of the alternative BPA design exploiting a bowtie outline.

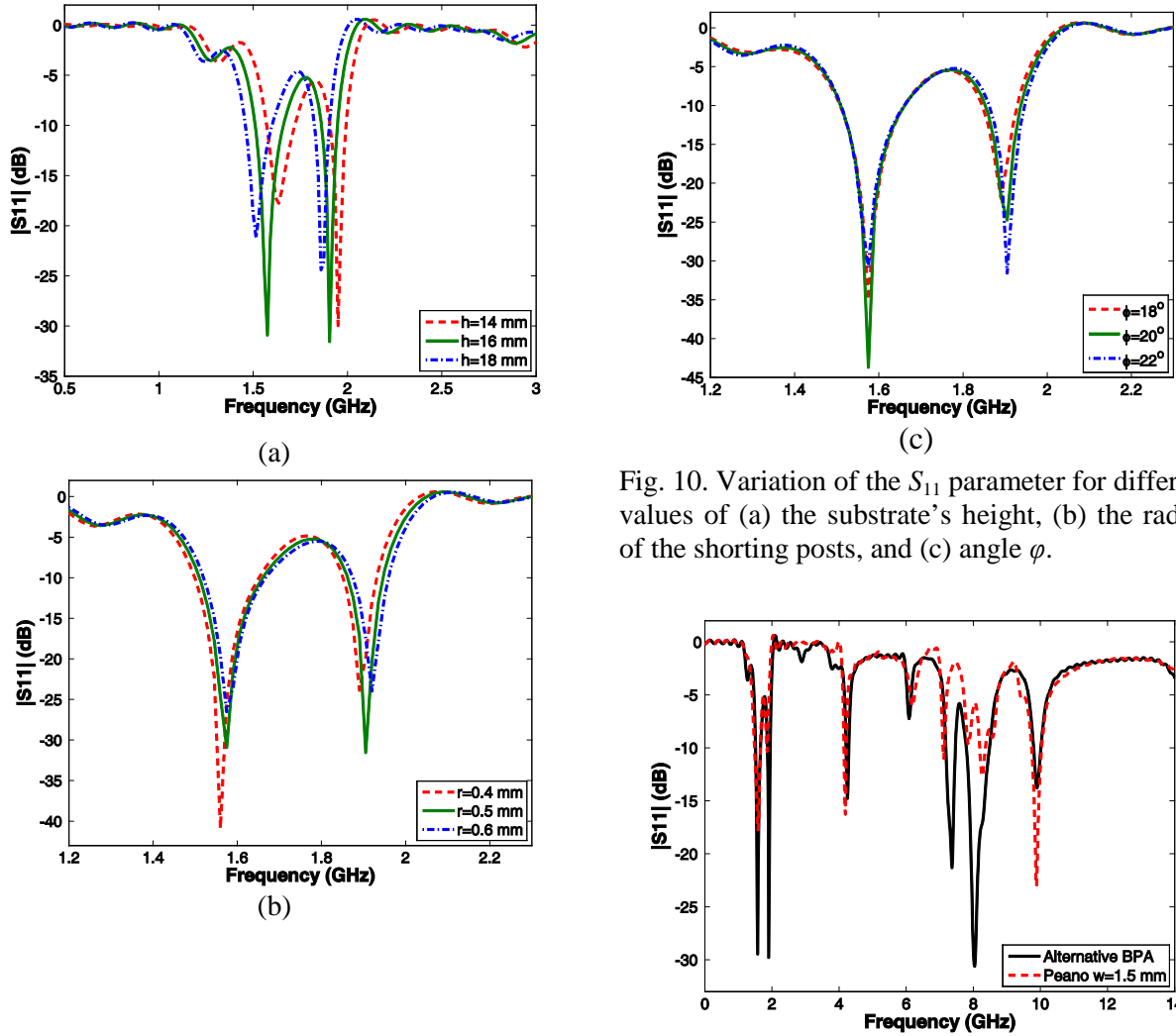


Fig. 10. Variation of the  $S_{11}$  parameter for different values of (a) the substrate's height, (b) the radius of the shorting posts, and (c) angle  $\phi$ .

Fig. 11. Variation of the  $S_{11}$  parameter: Conventional Peano design versus the alternative BPA.

Table 2: Radiation and spectral comparison (at -10 dB) of the Peano antenna and the alternative BPA

Antenna	Resonance	1st	2nd	3rd	4th	5th	6th	7th
Peano $w = 1.5$ mm	Frequency (GHz)	1.590	1.860	4.185	6.180	7.125	8.265	9.885
	Gain (dB)	3.5	3.0	5.1	7.9	8.8	7.8	7.5
	Bandwidth (GHz)	0.175	0.017	0.070	–	0.046	0.171	0.299
Alternative BPA	Frequency (GHz)	1.575	1.905	4.245	6.090	7.365	8.040	9.900
	Gain (dB)	4.6	4.2	6.8	8.4	9.9	10.2	7.8
	Bandwidth (GHz)	0.150	0.080	0.081	–	0.285	0.690	0.218

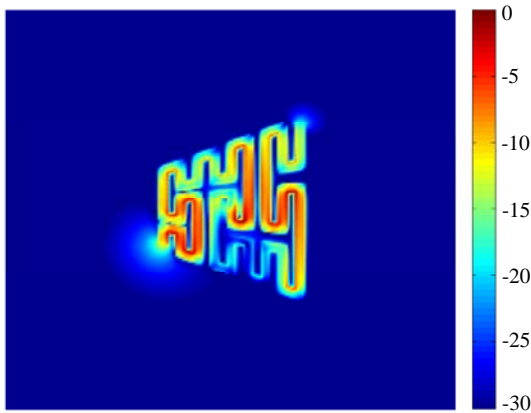


Fig. 12. Surface current distribution of the alternative BPA at 1.575 GHz.

### V. CONCLUSION

A new family of combined bowtie-Peano antennas with highly compact dimensions has been presented and comprehensively explored in this paper. The overall analysis verified a considerably enhanced operational bandwidth at certain resonances. Furthermore, a slight reduction in gain levels unveils a trade-off between the gain and the broadband behavior of the combined BPA. Nonetheless for the alternative BPA, a gain improvement at each resonance has been achieved, indicating that the proposed devices could be successfully incorporated in an assortment of modern miniaturized microwave implementations.

### ACKNOWLEDGMENT

This work was supported by the National Scholarships Foundation of Greece (IKY), under Grant No. 5282.

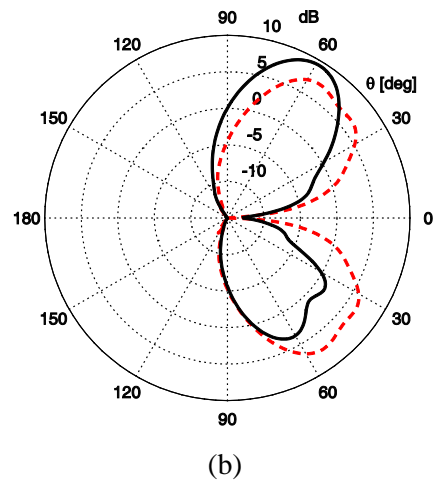
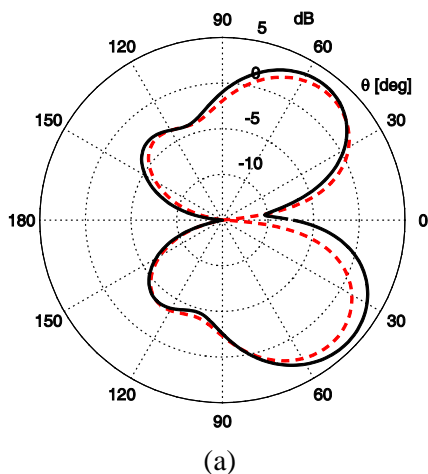


Fig. 13. Gain radiation patterns at  $\varphi = 135^\circ$  of conventional Peano design versus the alternative BPA: (a) Resonances at 1.86 GHz, 1.905 GHz, (red:  $w = 1.5$  mm, black: alternative BPA), and (b) resonances at 8.265 GHz, 8.04 GHz (red:  $w = 1.5$  mm, black: alternative BPA).

### REFERENCES

- [1] H. Sagan, *Space-Filling Curves*, Springer-Verlag, 1993.
- [2] J. Gonzalez-Arbesu, S. Blanch, and J. Romeu, "Are Space-Filling Curves Efficient Small Antennas?," *IEEE Antennas Wireless Propag. Lett.*, vol. 2, pp. 147-150, 2003.
- [3] R. Hasse, V. Demir, W. Hunsicker, D. Kajfez, and A. Elsherbeni, "Design and Analysis of Partitioned Square Loop Antennas," *Applied Computational Electromagnetic Society (ACES) Journal*, vol. 23, no. 1, pp. 53-61, 2008.
- [4] C. de J. van Coevorden, A. Bretones, M. Pantoja, S. Garcia, and A. Monorchio, "A New Implementation of the Hybrid Taguchi GA: Application to the Design of a Miniaturized Log-Periodic Thin-Wire Antenna," *Applied Computational Electromagnetic Society (ACES) Journal*, vol. 24, no. 1, pp. 21-31, 2009.
- [5] T. Spence, D. Werner, and J. Carvajal, "Modular Broadband Phased-Arrays Based on a Nonuniform Distribution of Elements Along the Peano-Gosper Space-Filling Curve," *IEEE Trans. Antennas Propag.*, vol. 58, no. 2, pp. 600-604, 2010.
- [6] S. Best, "A Comparison of the Resonant Properties of Small Space-Filling Fractal Antennas," *IEEE Antennas Wireless Propag. Lett.*, vol. 2, pp. 197-200, 2003.
- [7] J. McVay, A. Hoorfar, and N. Engheta, "Peano High Impedance Surfaces," *Radio Sci.*, vol. 40, pp. 1-9, 2005.
- [8] H. Oraizi and S. Hedayati, "Miniaturized UWB Monopole Microstrip Antenna Design by the

Combination of Giuseppe Peano and Sierpinski Carpet Fractals,” *IEEE Antennas Wireless Propag. Lett.*, vol. 10, pp. 67-70, 2011.

- [9] S.-H. Wi, J.-M. Kim, and J.-G. Yook, “Microstrip-Fed Bowtie-Shaped Meander Slot Antenna with Compact and Broadband Characteristics,” *Microw. Opt. Technol. Lett.*, vol. 45, no. 1, pp. 88-90, 2005.
- [10] J.-F. Li, B.-H. Sun, H.-J. Zhou, and Q.-Z. Liu, “Miniaturized Circularly-Polarized Antenna using Tapered Meander-Line Structure,” *PIERS*, vol. 78, pp. 321-388, 2008.
- [11] J. William and R. Nakkeeran, “A New UWB Slot Antenna with Rejection of WiMax and WLAN Bands,” *Applied Computational Electromagnetic Society (ACES) Journal*, vol. 25, no. 9, pp. 787-793, 2010.
- [12] E. El-Khouly, H. Ghali, and S. Khamis, “High Directivity Antenna using a Modified Peano Space-Filling Curve,” *IEEE Antennas Wireless Propag. Lett.*, vol. 6, pp. 405-407, 2007.
- [13] J. McVay, A. Hoorfar, and N. Engheta, “Space-Filling Curve Radio Frequency Identification Tags,” *Applied Computational Electromagnetic Society (ACES) Journal*, vol. 25, no. 6, pp. 517-529, 2010.
- [14] T. Terada, K. Ide, K. Iwata, and T. Fukusako, “Design of a Small, Low-Profile Print Antenna using a Peano Line,” *Microw. Opt. Technol. Lett.*, vol. 51, no. 8, pp. 1833-1838, 2009.
- [15] C. A. Balanis, *Modern Antenna Handbook*, Wiley-Blackwell, 2008.
- [16] A. Taflove and S. Hagness, *Computational Electrodynamics: The Finite-Difference Time-Domain Method*, Artech House, 2005.



**Ioannis I. Papadopoulos-Kelidis** received the Diploma degree in Electrical and Computer Engineering from the Aristotle University of Thessaloniki, Thessaloniki, Greece, in 2010. His research interests include computational electromagnetics and modern antenna design.



**Antonios X. Lalas** received the Diploma degree in Electrical and Computer Engineering from the Aristotle University of Thessaloniki, Thessaloniki, Greece, in 2006, where he is currently pursuing his Ph.D. degree. His research interests include computational electromagnetics and antenna design as well as the analysis and modeling of MEMS structures, with an emphasis on EBG and metamaterial applications.



**Nikolaos V. Kantartzis** received the Diploma and Ph.D. degrees from the Department of Electrical and Computer Engineering, Aristotle University of Thessaloniki, Greece, in 1994 and 1999, respectively. In 2001, he joined the same department, as a Postdoctoral Research Fellow, where, currently, he serves as an Assistant Professor. He has authored/co-authored 3 books, more than 55 refereed journal and over 70 conference papers. His main research interests include computational electromagnetics, contemporary antenna design, EMC modeling, higher-order time- and frequency-domain methods, metamaterials, and advanced microwave structures. Dr. Kantartzis is a member of diverse scientific societies and associations.



**Theodoros D. Tsiboukis** received the Diploma degree in Electrical and Mechanical Engineering from the National Technical University of Athens, Athens, Greece, in 1971, and the Doctor Eng. Degree from the Aristotle University of Thessaloniki (AUTH), Thessaloniki, Greece, in 1981. From 1981 to 1982, he was with the Electrical Engineering Department, University of Southampton, Southampton, U.K., as a Senior Research Fellow. Since 1982, he has been with the Department of Electrical and Computer Engineering, AUTH, where he is currently a Professor. He has served in numerous administrative positions and as a chairman of many conference organizing committees. He is the author of 8 books and over 250 refereed journal and conference papers. His research areas, primarily, focus on electromagnetic field analysis by energy methods, computational (frequency- and time-domain) electromagnetics, metamaterials and double-negative media, photonic crystals, inverse and EMC problems. Prof. Tsiboukis is a member of various societies, chambers, associations, and institutions, and has been the recipient of several awards and distinctions.